Subunit-Selective Contribution to Channel Gating of the M4 Domain of the Nicotinic Receptor

Cecilia Bouzat,* Fernanda Gumilar,* María del Carmen Esandi,* and Steven M. Sine†
*Instituto de Investigaciones Bioquímicas, UNS-CONICET, Bahía Blanca, Argentina; and †Receptor Biology Laboratory, Department of Physiology and Biophysics, Mayo Foundation, Rochester, MN, USA

ABSTRACT The muscle nicotinic receptor (AChR) is a pentamer of four different subunits, each of which contains four transmembrane domains (M1–M4). We recently showed that channel opening and closing rates of the AChR depend on a hydrogen bond involving a threonine at position 14′ of the M4 domain in the α-subunit. To determine whether residues in equivalent positions in non-α-subunits contribute to channel gating, we mutated δT14′, βT14′, and εS14′ and evaluated changes in the kinetics of acetylcholine-activated currents. The mutation εS14′A profoundly slows the rate of channel closing, an effect opposite to that produced by mutation of αT14′. Unlike mutations of αT14′, εS14′A does not affect the rate of channel opening. Mutations in δT14′ and βT14′ do not affect channel opening or closing kinetics, showing that conserved residues are not functionally equivalent in all subunits. Whereas αT14′A and εS14′A subunits contribute additively to the closing rate, they contribute nonadditively to the opening rate. Substitution of residues preserving the hydrogen bonding ability at position 14′ produce nearly normal gating kinetics. Thus, we identify subunit-specific contributions to channel gating of equivalent residues in M4 and elucidate the underlying mechanistic and structural bases.

INTRODUCTION

Nicotinic acetylcholine receptors are pentamers of homologous subunits. The primordial AChR pentamer likely contained only one type of subunit, exemplified by the α7 homopentamer found in brain. However, evolution led to subunit diversity and in parallel heteropentamers appeared. Presumably, fine tuning of subunit structure, together with combinatorial diversity of heteropentamers, allowed a wide range of physiological demands to be met. Therefore conserved residues in homologous subunits of heteropentamers potentially represent structures that contribute to particular physiological functions. Here we combine mutagenesis and single channel recordings to examine functional contributions of conserved residues in the M4 transmembrane domain of the heteromeric muscle AChR.

AChRs have the composition $\alpha_2\beta\varepsilon\delta$ in adult muscle and $\alpha_2\beta\gamma\delta$ in embryonic and denervated muscle. Each subunit contains an amino-terminal extracellular domain of ~210 amino acids, four transmembrane domains (M1–M4), and a short extracellular tail. Extracellular domains of four of the five subunits contribute to the two agonist binding sites where the biological response is initiated, whereas the M2 domain of each subunit contributes to the cation-selective channel, the endpoint of the biological response (Unwin, 1995). The locations and functional roles of the M1, M3, and M4 transmembrane domains are not as well understood as those of the M2 domain. However, together with M2 they likely comprise the channel gating apparatus.

The M4 domain is the least conserved among the transmembrane domains, is the most hydrophobic, and has been extensively labeled by hydrophobic probes (Blanton and Cohen, 1992, 1994). Although M4 is likely the outermost of the transmembrane domains, several findings suggest that it is essential for proper activation of the AChR (Bouzat et al., 1994; Lee et al., 1994; Ortiz-Miranda et al., 1997; Bouzat et al., 1998). We recently demonstrated that T422 located at position 14′ of the M4 domain of the α-subunit contributes through a hydrogen bond to channel gating (Bouzat et al., 2000). Here we combine site-directed mutagenesis with single-channel recordings to analyze the contribution to gating of this highly conserved residue in the M4 domain of the muscle non-α-subunits. Our studies reveal that the functional contribution of the residue at position 14′ is not conserved among the homologous subunits but is restricted to the α- and ε-subunits. Additionally, whereas in the α-subunit mutation of T14′ affects both channel opening and closing steps, mutations of the corresponding residue in the ε-subunit affects mainly the channel closing step.

MATERIALS AND METHODS

Construction of mutant subunits

Mouse cDNAs were subcloned into the cytomegalovirus-based expression vector pRBG4 (Sine, 1993). Mutant subunits were constructed using the QuikChange Site-Directed mutagenesis kit (Stratagene, La Jolla, CA). Restriction mapping and DNA sequencing confirmed all constructs.

Expression of AChR

HEK293 cells were transfected with α-, β-, δ-, and ε-cDNA subunits (wild-type or mutants) using calcium phosphate precipitation at a subunit

Submitted August 14, 2001, and accepted for publication December 14, 2001.

Address reprint requests to Dr. Cecilia Bouzat, Instituto de Investigaciones Bioquímicas, Camino La Carrindanga Km 7, 8000 Bahía Blanca, Argentina. Tel.: 54-291-486-1201; Fax: 54-291-486-1200; E-mail: inbouzat@criba.edu.ar.

0006-3495/02/04/1920/10 $2.00

TABLE 1 Mean values of open probability, open channel duration, and closed channel duration of clusters before and after the selection procedure

Subunit	[ACh] (μM)		Popen	Mean open duration (ms)	Mean closed duration (ms)	Number of events
Wild type	10	Before	0.10	0.88	7.02	4696
		After	0.10	0.82	7.36	4176
	30	Before	0.45	1.05	1.09	12,042
		After	0.47	1.02	1.11	11,148
	100	Before	0.86	0.91	0.12	8548
		After	0.85	0.83	0.12	7926
	300	Before	0.93	0.78	0.05	6406
		After	0.93	0.80	0.05	6006
εS14′A	10	Before	0.52	6.50	5.72	2630
		After	0.53	6.36	5.60	2393
	30	Before	0.88	8.02	1.03	2972
		After	0.89	8.41	0.97	2672
	100	Before	0.98	7.21	0.15	2300
		After	0.98	7.70	0.15	2090
	300	Before	0.98	6.33	0.08	4926
		After	0.98	6.32	0.08	4362

Mean values were obtained before and after the selection procedure from the open probability, mean open channel duration, and mean closed channel duration distributions of clusters corresponding to wild-type or εS14′A AChRs activated by different concentrations of ACh. Comparison of the mean values before and after selection indicates that the selected clusters are representative of all channels in the patch. Similar results were obtained for all recordings.

ratio of 2:1:1:1 for α:β:δ:ε, respectively, essentially as described previously (Bouzat et al., 1994, 1998). For transfections, cells at 40 to 50% confluence were incubated for 8 to 12 h at 37°C with the calcium phosphate precipitate containing the cDNAs in Dulbecco's Modified Eagle Medium (DMEM) plus 10% fetal bovine serum. Cells were used for single-channel measurements 1 or 2 days after transfection.

Patch-clamp recordings

Recordings were obtained in the cell-attached configuration (Hamill et al., 1981) at a membrane potential of −70 mV and at 20°C. The bath and pipette solutions contained 142 mM KCl, 5.4 mM NaCl, 1.8 mM $CaCl_2$, 1.7 mM $MgCl_2$, and 10 mM HEPES (pH 7.4). Patch pipettes were pulled from 7052 capillary tubes (Garner Glass Co, Claremont, CA) and coated with Sylgard (Dow Corning, Midland, MI). Acetylcholine (ACh) at final concentrations of 1 to 300 μM or 20 mM choline were added to the pipette solution.

Single-channel currents were recorded using an Axopatch 200B patch-clamp amplifier (Axon Instruments, Inc., Union City, CA), digitized at 5-μs intervals with the PCI-6111E interface (National Instruments, Austin, TX), recorded to the hard disk of a computer using the program Acquire (Bruxton Corporation, Seattle, WA), and detected by the half-amplitude threshold criterion using the program TAC (Bruxton Corporation, Seattle, WA) at a final bandwidth of 10 kHz. Data of AChRs activated by 20 mM choline were analyzed at a bandwidth of 5 kHz to avoid detection of some blockages that can be resolved at 10 kHz. Therefore, channel kinetics can be reduced to that of the closed to open reaction (Grosman and Auerbach, 2000). Open and closed time histograms were plotted using a logarithmic abscissa and a square root ordinate (Sigworth and Sine, 1987) and fitted to the sum of exponential functions by maximal likelihood using the program TACFit (Bruxton Corporation, Seattle, WA).

Open probability within clusters (p_{open}) was experimentally determined at each ACh concentration by calculating the mean fraction of time the channel is open within a cluster.

Kinetic analysis

Kinetic analysis was restricted to clusters of channel openings that each reflect the activity of a single AChR. Clusters of openings corresponding to a single channel were identified as a series of closely spaced events preceded and followed by closed intervals greater than a critical duration (ι_{crit}); this duration was taken as the point of intersection of the predominant closed component and the succeeding one in the closed time histogram. To minimize errors in assigning cluster boundaries, we analyzed only recordings from patches with low channel activity in which both components are clearly differentiated from one another. Because each cluster contains one more opening than closing, to avoid biasing in favor of opening, only clusters containing more than 10 openings were considered for further analysis. In addition, any clusters showing double openings were rejected. The predominant closed duration component, associated with closings within clusters, became shorter with increasing concentrations of agonist. Thus, we assume that this component reflects the set of transitions between unliganded closed and diliganded open states. Examples of the predominant closed component and the corresponding values of ι_{crit} for AChRs activated by different concentrations of ACh are: wild type, 10 μM, 6.50 ± 1.00 ms, ι_{crit} 40 to 50 ms; 30 μM, 1.10 ± 0.18 ms, ι_{crit} 8 to 10 ms; 100 μM, 0.18 ± 0.09 ms, ι_{crit} 1 to 1.5 ms; 300 μM, 0.08 ± 0.05 ms, ι_{crit} 0.8 ms; εS14′A, 10 μM, 4.90 ± 1.00 ms, ι_{crit} 40 to 50 ms; 30 μM, 1.20 ± 0.09 ms, ι_{crit} 8 to 10 ms; 100 μM, 0.23 ± 0.08 ms, ι_{crit} 1 to 1.5 ms; 300 μM, 0.09 ± 0.04 ms, ι_{crit} 0.8 ms; αT14′A, 30 μM, 4.40 ± 0.50 ms, ι_{crit} 40 to 50 ms; 100 μM, 0.86 ± 0.13 ms, ι_{crit} 10 to 15 ms; 300 μM, 0.38 ± 0.12 ms, ι_{crit} 2 to 3 ms; 600 μM, 0.13 ± 0.02 ms, ι_{crit} 1 ms.

For each recording, kinetic homogeneity was determined by selecting clusters on the basis of their distribution of mean open duration and p_{open}, as described before (Wang et al., 1997; Bouzat et al., 2000). For each cluster within a recording, we calculated the p_{open}, mean open duration, and mean closed duration and plotted their distributions. Typically, the distributions contained a dominant approximately Gaussian component and minor contributions of clusters with different properties. Clusters showing mean open duration and open probability values within 2 SD of the major component were selected and retained for the kinetic analysis. Typically, more than 80% of the events were selected (see Table 1). As shown in the examples of Table 1, mean values obtained from distributions of open probability, mean open channel duration, and mean closed channel duration of clusters do not change significantly after the selection procedure. In addition, comparison of closed- and open-time histograms before and after selection indicates that the selected clusters are representative of the predominant population of AChR in the patch (Bouzat et al., 2000).

The resulting open and closed intervals from different patches, each at a specified ACh concentration or at 20 mM choline, were analyzed according to kinetic schemes using the program MIL (QuB suite, State University of New York, Buffalo, NY). Briefly, the program allows simultaneous fitting of recordings at different agonist concentrations and estimates the rate constants using a maximal likelihood method that corrects for missed events (Qin et al., 1996). The dead time was typically 30 μs; calculated rate constants were stable over a range of dead times varying from 18 to 40 μs (Bouzat et al., 2000). Probability density functions of open and closed durations were calculated from the fitted rate constants and instrumentation dead time and superimposed on the experimental dwell time histogram as described by Qin et al. (1996). Calculated rates were accepted only if the resulting probability density functions correctly fitted the experimental open and closed duration histograms.

For wild-type and some mutant AChRs activated by ACh, β_2 was constrained to its previously estimated value (Sine et al., 1995; Wang et al., 1997; Salamone et al., 1999) because brief closings due to gating and channel blocking become indistinguishable at high ACh concentrations (Wang et al., 1997; Salamone et al., 1999; Bouzat et al., 2000). When β_2 was allowed to vary freely, MIL failed to converge to a well-defined set of rate constants and approached a value of $\sim$100,000 s^{-1} (Salamone et al., 1999; Bouzat et al., 2000). Additionally, association and dissociation rate constants were assumed to be equal at both binding sites (Akk and Auerbach, 1996; Wang et al., 1997; Salamone et al., 1999). Rate constants are shown with standard deviations.

RESULTS

Analysis of M4 mutant AChRs

We previously demonstrated that αT14′ forms a hydrogen bond essential for proper rates of channel opening and closing (Bouzat et al., 2000). To further examine functional contributions of the equivalent residues in the non-α-subunits, we replaced the conserved threonines in β- and δ-subunits by alanine and serine, as well as the equivalent serine in the ε-subunit by threonine and alanine. We transfected HEK 293 cells with mutant plus wild-type subunit cDNAs and recorded single channel currents activated by a range of desensitizing concentrations of ACh (3–300 μM). At these ACh concentrations, single channel currents activate in clear clusters of events corresponding to a single channel (Sakmann et al., 1980).

Cotransfection of HEK 293 cells with mutant and wild-type subunit cDNAs could result in the surface expression of subunit-omitted AChRs. However, omitting the β- or δ-subunits eliminates all cell-surface expression. Omitting the ε-subunit reduces the surface expression to only 16 to 20% of that of $\alpha_2\beta\varepsilon\delta$ pentamers. In addition, channel activity of $\alpha_2\beta\delta_2$ pentamers is difficult to detect (Bouzat et al., 1994; Engel et al., 1996). In contrast, channel activity from all mutant AChRs in this study was as easily detected as that from wild-type $\alpha_2\beta\varepsilon\delta$ AChRs. Furthermore, surface expression of each of the mutant AChRs was similar to that of wild-type AChRs. Thus subunit-omitted receptors do not contaminate recordings from our mutant AChRs.

Wild-type as well as all mutant AChRs open in clusters of well-defined activation episodes at ACh concentrations greater than 3 μM. Single-channel recordings from AChRs containing subunits mutated at position 14′ show that only mutations in α- and ε-subunits affect gating kinetics (Fig. 1). We previously reported that the mutant αT14′A AChR shows both briefer openings and prolonged intracluster closings compared to wild-type AChRs (Bouzat et al., 2000). By contrast, AChRs containing the mutant εS14′A subunit show greatly prolonged openings, opposite to αT14′A. AChRs containing the mutant βT14′A and δT14′A subunits exhibit open and closed intervals similar to wild-type AChRs (Fig. 1 and Table 2).

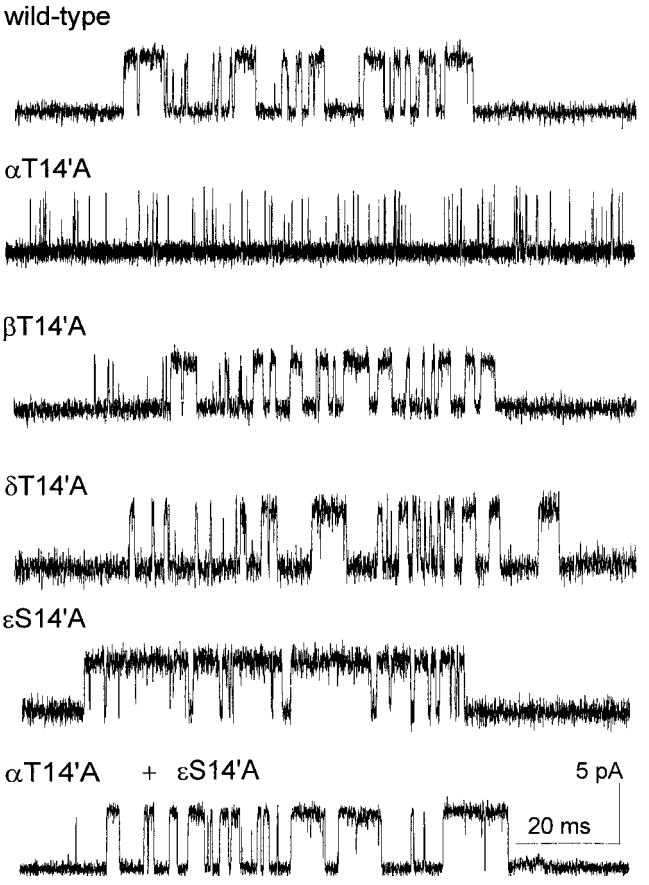

FIGURE 1 Clusters of single-channel currents from wild-type and mutant AChRs. Channels activated by 30 μM ACh were recorded from HEK cells expressing mouse wild-type ($\alpha_2\beta\varepsilon\delta$) and AChRs carrying the mutant subunits (αT14′A, βT14′A, δT14′A, εS14′A, and αT14′A plus εS14′A). Currents are displayed at a bandwidth of 9 kHz with channel openings as upward deflections. Membrane potential: −70 mV.

Histograms of open intervals exhibit a main component with a mean of $\sim$900 μs for wild-type AChRs (Table 2). The mean duration of this component decreases by an order of magnitude in the mutant αT14′A AChR, whereas it increases by an order of magnitude in the εS14′A mutant (Table 2). Maintaining hydrogen bonding capability of the side chain with the αT14′S and εS14′T mutations retains normal open intervals (Table 2). Histograms of open intervals for AChRs containing the mutations βT14′A and

TABLE 2 Channel properties of adult AChRs carrying mutations in the M4 domain

Subunit	O_1 (ms)	(Area)	O_2 (ms)	C_1 (ms)
Wild type	0.90 ± 0.08	0.90 ± 0.18	0.20 ± 0.06	1.10 ± 0.18
αT14′A	0.12 ± 0.04	0.70 ± 0.06	0.35 ± 0.05	4.40 ± 0.50
αT14′S	0.70 ± 0.07	0.56 ± 0.10	0.20 ± 0.05	1.70 ± 0.70
εS14′A	9.80 ± 0.80	0.87 ± 0.05	0.40 ± 0.10	1.20 ± 0.09
εS14′T	0.78 ± 0.20	1.00 ± 0.00		1.50 ± 0.15
βT14′A	0.80 ± 0.20	0.60 ± 0.05	0.20 ± 0.06	1.60 ± 0.40
βT14′S	0.96 ± 0.30	0.60 ± 0.02	0.27 ± 0.04	2.00 ± 0.40
δT14′A	0.70 ± 0.20	0.90 ± 0.05	0.14 ± 0.04	1.75 ± 0.50
δT14′S	0.66 ± 0.20	0.70 ± 0.05	0.22 ± 0.10	2.75 ± 0.60
αT14′A + εS14′A	1.30 ± 0.20	0.80 ± 0.05	0.13 ± 0.02	3.60 ± 0.90

Recordings were obtained at a membrane potential of −70 mV from HEK cells transfected with wild-type and the specified mutant subunits. ACh concentration, 30 μM. Values were obtained from the open and closed-time histograms. O_1 corresponds to the main component of the open time histogram. C_1 corresponds to the intracluster closed component, which is sensitive to ACh concentration. Data are expressed as the mean ± SD of at least three different experiments.

δT14′A AChRs are indistinguishable from that of wild-type AChR; similar results were obtained with the corresponding mutations to serine in the β and δ subunits (Table 2). Thus, substitutions at position 14′ of M4 of all subunits that preserve the hydrogen bonding ability do not affect channel open intervals.

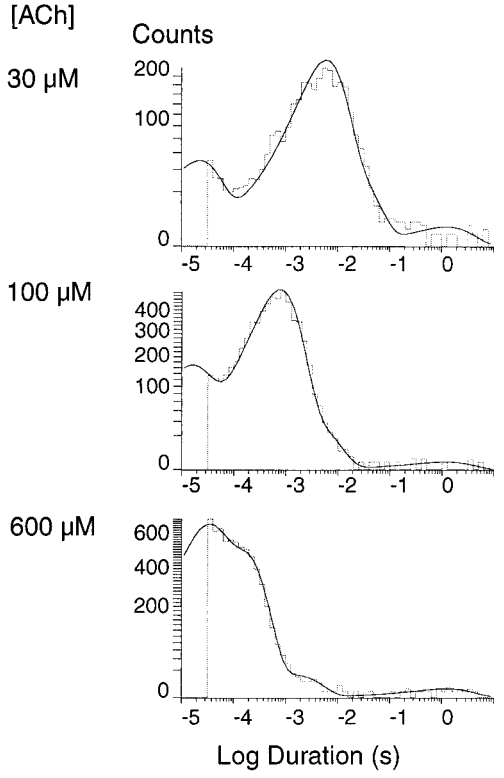

FIGURE 2 Closed time histograms of αT14′A AChRs activated by different ACh concentrations. Mutant AChR channels were activated by a given ACh concentration. The predominant closed duration component, associated with closings within clusters, becomes shorter with increasing concentrations of agonist. This component reflects the set of transitions between unliganded closed and diliganded open states.

For both wild-type and mutant AChRs, histograms of closed intervals within clusters show a main component that becomes progressively briefer with increasing ACh concentration. Fig. 2 clearly illustrates the dependence of the duration of this component on agonist concentration in the αT422A AChR. This main component reflects the set of transitions between unliganded closed and diliganded open states. We previously reported that for the αT14′A mutant, the mean for this component greatly exceeds that of wild-type AChR at all agonist concentrations (Bouzat et al., 2000; Fig. 1 and Table 2). On the contrary, for the εS14′A, βT14′A, and δT14′A mutants, the mean closed duration at a given agonist concentration is similar to that of wild-type AChR (Fig. 1 and Table 2). Again, substitutions preserving the hydrogen bond ability at position 14′ of all subunits do not affect distributions of closed intervals.

Given that open intervals decrease in the αT14′A mutant but increase in the εS14′A mutant, we investigated the effect of combining both mutant subunits in a single AChR. Open intervals for receptors containing both mutations are similar to those of wild type (Fig. 1 and Table 2). Thus, the opposing effects of αT14′A and εS14′A offset each other when present in the same AChR. Because the two αT14′ residues contribute additively to the duration of the open state (Bouzat et al., 1998), the effect of mutating the ε subunit is approximately twice that of mutating the α subunit. On the other hand, closed intervals are slightly prolonged in the double mutant compared to wild-type AChR (Table 2).

Kinetic analysis of M4 mutant AChRs

To identify the kinetic step affected by the mutant subunits and to quantify the kinetic changes, we fitted the classical activation scheme (Scheme 1) to the open and closed dwell times.

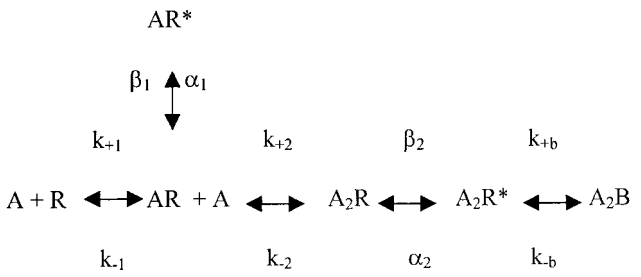

Scheme 1.

In Scheme 1, two agonists (A) bind to receptors (R) in the resting state with association rates k_{+1} and k_{+2} and dissociate with rates k_{-1} and k_{-2}. Receptors occupied by one agonist open with rate β_1 and close with rate α_1, and AChRs occupied by two agonists open with rate β_2 and close with rate α_2. At high agonist concentrations (greater than 100 μM ACh) channel blockade is evident and thus the blocked state, A_2B, is included. To estimate the set of rate constants, Scheme 1 was fitted to the data using the program MIL (Qin et al., 1996). We analyzed recordings obtained at multiple ACh concentrations (10–300 μM) simultaneously with the aim of representing sojourns in all the states in Scheme 1 in the analysis.

Rate constant estimates obtained for wild-type AChR (Fig. 3 and Table 3) agree with those previously reported for mouse AChR (Wang et al., 1997; Salamone et al., 1999; Bouzat et al., 2000). Data for all mutants are also well described by Scheme 1 (Fig. 3). The fitted rate constants reveal that the mutation εS14′A markedly slows the rate of channel closing (Table 3). In addition, small changes in association and dissociation rate constants are observed in this mutant AChR. In contrast, the corresponding mutations in the β- and δ-subunits do not affect activation rate constants (Fig. 3 and Table 3). Thus, the amino acid located at position 14′ of M4 contributes mainly to channel opening and closing rates in the α-subunit (Bouzat et al., 2000), to the channel closing rate in the ε-subunit, but does not contribute to channel gating in the β- and δ-subunits.

When both mutant α- and ε-subunits are combined into a single AChR, the resulting channels activate with kinetics similar to wild-type AChR. Kinetic analysis of the double mutant AChR reveals normal rate constants except for a slight slowing in the rate of channel opening (Fig. 3 and Table 3). For this mutant, data could be well-fitted allowing β_2 to vary freely (Table 3). Thus, our results show that residue 14′ in M4 of the α- and ε-subunits contributes additively to the channel closing rate but contributes non-additively to the channel opening rate.

Activation of AChRs by choline

Because the channel opening rate constant for wild-type AChRs activated by ACh approaches the time resolution limits of the patch clamp, and because the εS14′A mutation increases the probability of channel opening (see below), we used choline, an agonist with a very slow opening rate, to test the possibility that εS14′A affects the rate of channel opening (Grosman and Auerbach, 2000). At 20 mM choline, openings occur in easily recognizable clusters for both wild-type and mutant AChRs. Open-channel blockade elicited by the high concentration of choline appears as a reduction in channel amplitude (Grosman and Auerbach, 2000). The mean current of 20 mM choline-activated channels, 2.6 ± 0.3 pA, is ~50% lower than that of AChRs activated by 1 to 100 μM ACh (5.5 ± 0.3 pA) or 100 μM choline (5.6 ± 0.5 pA).

For both wild-type and mutant choline-activated AChRs, open time histograms are well described by a single exponential, but the mean durations differ by approximately an order of magnitude as observed for ACh (0.45 ± 0.07 ms and 3.40 ± 0.70 ms for wild-type and εS14′A AChRs, respectively). Closed time histograms for the choline-activated AChRs show a main component that corresponds to intracluster closings (mean durations are 17 ± 3 ms and 11 ± 2 ms for wild-type and εS14′A AChRs, respectively). To analyze the kinetics of channel opening and closing in the presence of 20 mM choline, we fitted Scheme 2 to the closed and open intervals of the selected clusters.

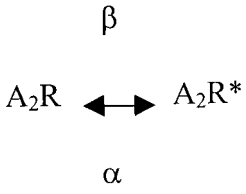

Scheme 2.

Scheme 2 is a subset of Scheme 1, which reduces the kinetics of AChR activity to the closed to open transition because 20 mM choline is a saturating agonist concentration (Grosman and Auerbach, 2000). The resulting estimates for opening and closing rate constants are: wild-type, 110 ± 10 s^{-1} and 2200 ± 50 s^{-1} for β and α, respectively; εS14′A AChR, 125 ± 3 s^{-1} and 285 ± 7 s^{-1} for β and α, respectively. Thus the changes in gating rate constants using choline as the agonist agree with those using ACh, indicating that εS14′ selectively affects the channel closing step.

Changes in free energy and double mutant cycles analysis

The channel gating equilibrium constant for ACh-activated receptors, θ, calculated as β_2/α_2, increases approximately sixfold in the εS14′A mutant compared to wild type (θ =

33), whereas it decreases 20-fold in the αT14′A mutant, indicating opposite and unequal contributions of the α- and ε-subunits to the gating equilibrium. Interestingly, when both mutant subunits are combined, the gating equilibrium is close to that of the wild-type AChR (Table 4). Table 4 shows that compared with wild-type AChR, the free energy change of the gating equilibrium is twofold greater in the αT14′A than in the εS14′A AChR. However, if each α-subunit of the AChR contributed equally to the gating equilibrium, the free energy changes would be equal for both α- and ε-subunits.

To determine the degree of coupling between residues at positions 14′ of α-and ε-subunits, we used thermodynamic mutant cycles to analyze the gating equilibrium (Horovitz and Fersht, 1990; Hidalgo and MacKinnon, 1995). Our mutational analysis can be described by the following pair of joined mutant cycles:

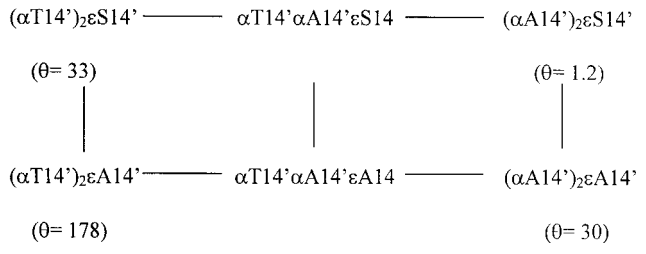

Scheme 3.

The cycle begins in the upper left corner containing the wild-type AChR and ends in the lower right corner with mutations in all three subunits. We do not analyze the steps indicating one mutant α-subunit because of the problem of separating kinetically different types of AChRs after coexpression of both wild-type and mutant α-subunits (Bouzat et al., 1998). Thus, our measured free-energy change upon mutating the α-subunit corresponds to the sum of the two horizontal steps in the cycle. Based on this cycle, we calculated a coupling coefficient Ω according to:

$$\Omega = \theta(\mathrm{wt}) \times \theta(\alpha_{\mathrm{A14'}}\varepsilon_{\mathrm{A14'}})/\theta(\alpha_{wt}\varepsilon_{\mathrm{A14'}}\varepsilon_{\mathrm{wt}}) = 4.6$$

which corresponds to a coupling free energy (RT ln Ω) of ~0.8 kcal/mol.

We also calculated the contribution of residue 14′ to activation free energies for the closed to open transition and for the open to closed transition. Changes of activation free energies due to the mutations could result from changes in ground or transition states or both. Whereas the mutation in the ε-subunit increases the free energy for channel closing, the mutation in the α-subunit decreases it to a similar extent (Table 4). No changes in activation-free energies for channel closing are observed when both mutant subunits are combined (Table 4). As described for the gating equilibrium, assuming that each α-subunit contributes equally to closing and opening steps, our results indicate that the ε-subunit affects the closing transition to a greater extent than the α-subunit. In contrast, whereas the activation free energy for channel opening is increased in the α-mutant, it is unchanged in the εA14′ AChR (Table 4).

Open probability of M4 mutant AChRs

To determine the overall consequences of each mutation for receptor activation we determined the open probability as a function of ACh concentration and compared it with that predicted by the kinetically determined rate constants. The predicted dose-response curves superimpose upon the open probability measurements, supporting the estimated rate constants (Fig. 4). For wild-type AChRs, open probability increases with increasing ACh concentration, showing an EC_{50} of 40 μM. As described before, the dose-response curve of the mutant αT14′A AChR is displaced to higher ACh concentrations owing to impaired channel gating (Bouzat et al., 2000). In contrast, the curve for εS14′A-containing AChRs is shifted to lower ACh concentrations, decreasing the EC_{50} to 9 μM. As expected, the profiles for the βT14′A (EC_{50} = 58 μM), δT14′A (EC_{50} = 46 μM), as well as that for the double mutant αT14′A-εS14′A AChRs (EC_{50} = 57 μM) are similar to that of the wild-type AChR (Fig. 4).

DISCUSSION

Although M4 is the least conserved of the four transmembrane domains, T14′ is highly conserved among subunits and species. We previously demonstrated that in the α subunit a hydrogen bond involving the side chain at position 14′ contributes to rapid and efficient gating of the muscle AChR. Here we determine whether these structural and mechanistic contributions to gating are conferred by non-α-subunits. The results indicate that the functional contribution of the residue at position 14′ of M4 is restricted to the α- and ε-subunits, showing that at this position sequence identity among subunits is not accompanied by a common functional contribution.

The present kinetic analysis shows no changes due to mutation at position 14′ in β- and δ-subunits. In contrast, mutation of position 14′ in the ε-subunit profoundly slows the step underlying channel closing. Interestingly, this effect is quantitatively opposite to that observed for the αT14′A AChR. When mutations in the α- and ε-subunits are combined in a single receptor, the resulting closing rate is similar to that of wild-type AChR. Thus, mutations in α- and ε-subunits contribute additively to the rate of channel closing. Because each AChR contains two αT14′ residues, and because both α-subunits contribute additively and equally to the closing rate (Bouzat et al., 1998), the present

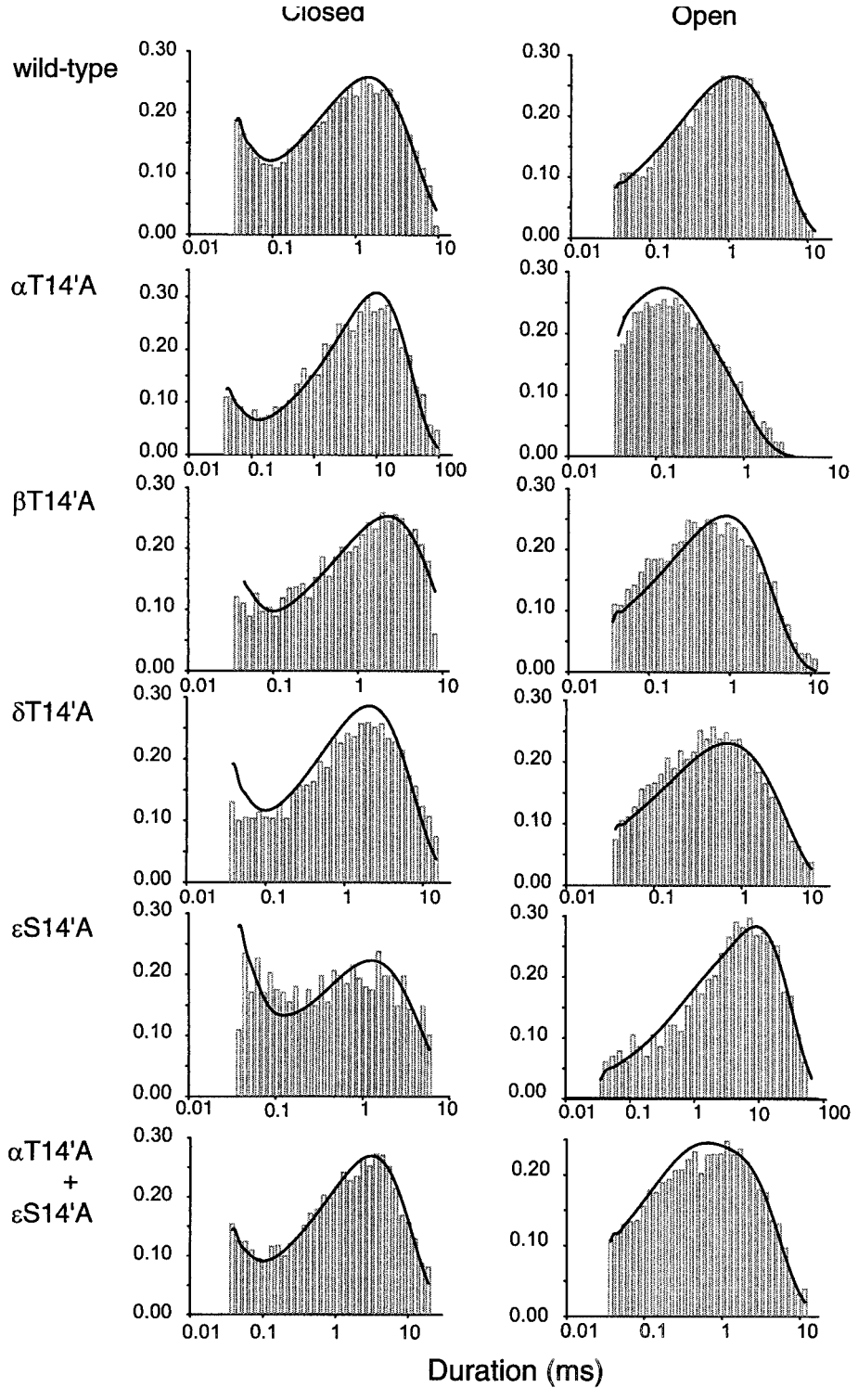

FIGURE 3 Kinetics of activation of wild-type and mutant AChRs. Open and closed-time histograms of wild-type and mutant AChRs containing the indicated mutant subunit(s) with the fit for Scheme 1 superimposed to the experimental data. Histograms were constructed with the selected clusters. The ordinates correspond to the square root of the fraction of events per bin. The fitting was performed simultaneously with a range of ACh concentrations (3–300 μM) for each mutant. The data shown correspond to 30 μM ACh.

results indicate that the residue at 14′ of the ε-subunit has a greater effect on the channel closing rate than that of the α-subunit.

The channel opening rate is affected differently by mutations in the α- and ε-subunits. Channel opening is slowed in the αT14′A mutant AChR, as revealed by prolonged

TABLE 3 Kinetic parameters for mouse wild-type and AChRs mutated at position 14′ of M4

	k_{+1}	k_{-1}	k_{+2}	k_{-2}	β_1	α_1	β_2	α_2	k_{+b}	k_{-b}
WT	330	28,000	170	56,000	640	2600	50,000	1500	9	78,000
	±40	±2500	±20	±5000	±40	±140		±100	±1	±6000
εS14′A	240	12,000	120	24,000	140	1000	50,000	280	2	78,000
	±12	±600	±5	±1200	±30	±370		±10	±1	
δT14′A	280	26,000	140	51,000	600	3500	50,000	2400	13	78,000
	±10	±1100	±5	±2200	±50	±200		±90	±2	
βT14′A	320	30,600	160	54,700	122	4900	50,000	2080	14	78,000
	±15	±1800	±7	±2400	±24	±500		±70	±4	
αT14′A	250	27,600	120	55,300			12,800	10,400	57	78,000
	±10	±1300	±5	±2500			±400	±180	±5	
αT14′A + εS14′A	240	31,000	120	62,000	800	3500	36,000	1200	5	78,000
	±15	±2200	±10	±4400	±100	±300	±4900	±70	±1	

Rate constants are in units of $\mu M^{-1}\ s^{-1}$ for association rate constants and s^{-1} for all others. Values are results of a global fit of Scheme 1 to data obtained over a range of concentration of ACh. Standard deviations are shown. Data without showing standard errors have been constrained to allow a better fit. The data of the αT14′A mutant were obtained from Bouzat et al. (2000).

closings within clusters at high ACh concentrations (Fig. 1) and channel closing is accelerated (Table 3). In addition, data for the αT14′A AChR are not well described by Scheme 1. Instead, activation is described by a kinetic scheme containing two consecutive doubly liganded open states (Bouzat et al., 2000). This scheme was previously used to describe activation of other mutant AChRs, which also showed slower rates of channel opening (Wang et al., 1999). Thus, consecutive double liganded open states may be present but not distinguished in wild-type AChRs because the observed rate of channel closing is relatively rapid.

Recordings obtained in the presence of ACh show that the equivalent mutation in the ε-subunit, εS14′A, does not change the rate of channel opening. Because the opening rate constant of wild-type AChRs (β_2 in Scheme 1) is at the upper limit of reliable estimation, even a modest increase makes this parameter too fast to be resolved (Grosman and Auerbach, 2000). Therefore, we study the opening rate of εS14′A channels activated by saturating concentrations of a slowly opening, low-efficacious agonist as choline. At a saturating concentration of choline, the kinetics of the channel can be reduced to that of the closed to open reaction. Because the opening rate, β, is slow in the choline-activated AChRs, this constant can be well measured and thus an increase in such constant can be easily detected. The calculated values for closing and opening rates of wild-type AChRs activated by choline generally agree with those previously reported (Grosman and Auerbach, 2000). The calculated opening rate constant for εS14′A mutant is similar to that of wild-type AChR. Thus, in contrast to mutations in the α subunit, which affect both the opening and closing steps, the mutation in the ε subunit selectively affects the closing step.

TABLE 4 Differences in free energy of channel gating and opening and closing reactions

Subunit	θ	Gating Δ(ΔG)	Closing Δ(ΔG)	Opening Δ(ΔG)
εS14′A	178	−0.96	1.02	0
αT14′A	1.23	1.90	−1.20	0.70
αT14′A + εS14′A	30	−0.05	0.10	0.18

θ is the diliganded gating equilibrium constant (β_2/α_2). Values of opening (β_2) and closing (α_2) rates were obtained from Table 3.

Δ(ΔG) for closing and opening are the changes between mutant (m) and wild-type AChRs (w) in the energy that the channel must overcome to make the transition from the biliganded open to the closed state (closing) and from this to the open state (opening).

The differences in free energy are calculated as $\Delta(\Delta G)$ (kcal/mol) $= -RT \ln \theta m/\theta wt$ for gating, $\Delta(\Delta G) = -RT \ln \alpha_2 m/\alpha_2 wt$ for closing, and $\Delta(\Delta G) = -RT \ln \beta_2 m/\beta_2 wt$ for opening. R is the gas constant and T is the absolute temperature.

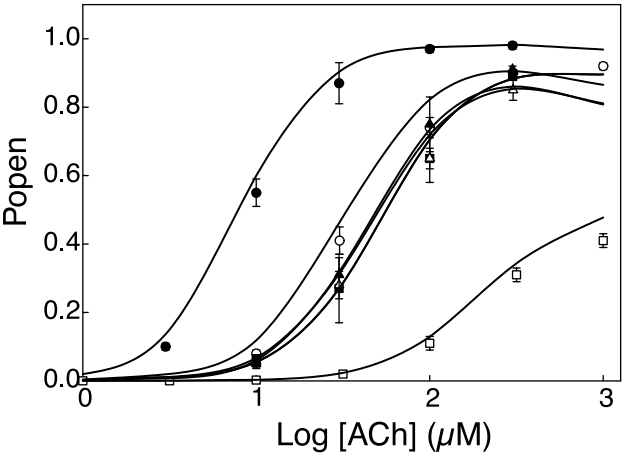

FIGURE 4 Agonist concentration dependence of the channel open probability. The mean fraction of time the channel is open during a cluster (p_{open}) was experimentally determined at the indicated concentrations of ACh. Each point corresponds to the mean ± SD of three patches. The symbols correspond to: ○, wild type; ●, εS14′A; □, αT14′A; ■, αT14′A + εS14′A; △, βT14′A; ▲, δT14′A. The curves were calculated from Scheme 1, using the fitted rate constants in Table 3, and superimposed on the experimentally determined p_{open} values.

The extent of coupling between different mutant residues can be quantified using double mutant cycles analysis (Horovitz and Fersht, 1990). Applied to the channel gating equilibrium, mutations of residue 14′ in the α- and ε-mutants show a low coupling free energy of 0.8 kcal/mol, indicating nearly independent contributions of the mutant subunits. However, to obtain purely independent contributions of both mutant subunits to the gating equilibrium, the opening rate of the εS14′A AChR should be ~230,000 s^{-1} rather than the observed 50,000 s^{-1}. Alternatively, the opening rate for the double mutant, which was 36,000 s^{-1}, should approach the 12,000 s^{-1} observed for the αT14′A AChR. Either of these expected opening rates should have been easily detected in our experiments. Thus the α- and ε-subunits appear to be weakly coupled in contributing to the channel gating equilibrium. Because the α- and ε-subunits contribute additively to the closing rate, and because the closing rate of the double mutant is similar to that of the wild-type AChR, coupling between subunits appears to originate in the channel opening step.

The apparent coupling between α- and ε-subunits may owe to a selective effect of the mutations on ground versus transition state free energies. The double mutant AChR (αT14′A plus εS14′A) shows a slight decrease in the opening rate constant compared to wild type. However, the rate constant for the double mutant is significantly greater than that of the αT14′A AChR. Also, in contrast to the α-mutant AChR, activation of the double mutant receptor can be well described by Scheme 1. These results indicate that the εS14′A subunit by itself does not affect the opening rate, but when combined with the αT14′A mutant subunit, it counteracts the profound decrease in opening rate due to the αT14′A mutation. A possible explanation is that the εS14′A mutation affects free energy of the closed ground state and the transition state to similar extents, which would not affect the rate constant for opening. The αT14′A mutant, on the other hand, may stabilize the closed ground state, leaving the transition state unaffected, which would slow the rate of opening. However, when the mutant ε subunit is combined with the mutant α-subunit, the combination of effects on ground and transition states leads to an intermediate rate of channel opening.

Our results also reveal the structural basis of the contribution of this lipid-exposed residue in M4 to channel gating. Substitution to threonine in the ε-subunit, which preserves the hydrogen bonding ability of the side chain, does not affect gating kinetics. In addition, the free energy changes for channel closing are in the range expected for hydrogen bonds between uncharged residues in an aqueous solution (0.5–1.5 kcal/mol; Fersht et al., 1985). Together with our previous analysis of αT14′ (Bouzat et al., 2000), the present results suggest that although the functional contributions to channel gating of the εS14′ and αT14′ are different, the structural bases are common, in both cases mediated by a hydrogen bond.

One explanation for the subunit-selective function of the side chain at position 14′ of M4 is that the orientation of this highly conserved residue differs among the subunits. In this regard, T14′ in M4 has been labeled by 3-trifluoromethyl-3-(*m*-iodophenyl)diazirine (TID) in the α-subunit of *Torpedo,* suggesting that it is situated at the lipid-protein interface of the AChR. However, the equivalent residues in β-, δ-, and γ-subunits were not labeled by TID (Blanton and Cohen, 1994). An alternative explanation is based on the key role that the ε-subunit plays in governing gating kinetics. In this respect, it is responsible for the fast kinetics typical of the adult AChR. Moreover, we previously showed that residues in the HA region, located within the M3-M4 intracellular domain, together with residues in M4 underlie the different open durations between ε- and γ-containing AChRs (Bouzat et al., 1994). Thus, the unique functional roles of the α- and ε-subunits could also explain the subunit-specific contributions to gating of residue at 14′ position of the M4 domain.

This work was supported by grants from Ministerio de Salud de la Nación, Universidad Nacional del Sur, Agencia Nacional de Promoción Científica y Tecnológica to C.B. and FIC grant 1R03 TW01185-01 to S.M.S. and C.B.

REFERENCES

Akk, G., and A. Auerbach. 1996. Inorganic, monovalent cations compete with agonists for the transmitter binding site of nicotinic acetylcholine receptors. *Biophys. J.* 70:2652–2658.

Blanton, M. P., and J. B. Cohen. 1992. Mapping the lipid-exposed regions in the *Torpedo californica* nicotinic acetylcholine receptor. *Biochemistry.* 31:3738–3750.

Blanton, M. P., and J. B. Cohen. 1994. Identifying the lipid-protein interface of the *Torpedo* nicotinic acetylcholine receptor: secondary structure implications. *Biochemistry.* 33:2859–2872.

Bouzat, C., F. J. Barrantes, and S. M. Sine. 2000. Nicotinic receptor fourth transmembrane domain: hydrogen bonding by conserved threonine contributes to channel gating kinetics. *J. Gen. Physiol.* 115:663–672.

Bouzat, C., N. Bren, and S. M. Sine. 1994. Structural basis of the different gating kinetics of fetal and adult nicotinic acetylcholine receptors. *Neuron.* 13:1395–1402.

Bouzat, C., A. M. Roccamo, I. Garbus, and F. J. Barrantes. 1998. Mutations at lipid-exposed residues of the acetylcholine receptor affect its gating kinetics. *Mol. Pharmacol.* 54:146–153.

Engel, A. G., K. Ohno, C. Bouzat, S. M. Sine, and R. C. Griggs. 1996. End-plate acetylcholine receptor deficiency due to nonsense mutations in the ε subunit. *Ann. Neurol.* 40:810–817.

Fersht, A. R., J.-P. Shi, J. Knill-Jone, D. M. Lowe, A. J. Wilkinson, D. M. Blow, P. Brick, P. Carter, M. M. Y. Waye, and G. Winter. 1985. Hydrogen bonding and biological specificity analyzed by protein engineering. *Nature.* 314:235–238.

Grosman, C., and A. Auerbach. 2000. Asymmetric and independent contribution of the second transmembrane segment 12′ residues to diliganded gating of acetylcholine receptor channels. *J. Gen. Physiol.* 115: 637–651.

Hamill, O. P., A. Marty, E. Neher, B. Sakmann, and F. J. Sigworth. 1981. Improved patch-clamp techniques for high-resolution current recording from cells and cell-free membrane patches. *Pflugers Arch.* 391:85–100.

Hidalgo, P., and R. MacKinnon. 1995. Revealing the architecture of a K+ channel pore through mutant cycles with a peptide inhibitor. *Science.* 268:307–310.

Horovitz, A., and A. R. Fersht. 1990. Strategy for analysing the cooperativity of intramolecular interactions in peptides and proteins. *J. Mol. Biol.* 214:613–617.

Lee, Y-H., L. Li, J. Lasalde, L. Rojas, M. McNamee, S. I. Ortiz-Miranda, and P. Pappone. 1994. Mutations in the M4 domain of *Torpedo californica* acetylcholine receptor dramatically alter ion channel function. *Biophys. J.* 66:646–653.

Ortiz-Miranda, S. I., J. A. Lasalde, P. A. Pappone, and M. G. McNamee. 1997. Mutations in the M4 domain of the *Torpedo californica* nicotinic acetylcholine receptor alter channel opening and closing. *Membr. Biol.* 158:17–30.

Qin, F. A., A. Auerbach, and F. Sachs. 1996. Estimating single-channel kinetic parametes from idealized patch clamp data containing missed events. *Biophys. J.* 70:264–280.

Sakmann, B. J., J. Patlak, and E. Neher. 1980. Single acetylcholine-activated channels show burst-kinetics in the presence of desensitizing concentrations of agonist. *Nature.* 286:71–73.

Salamone, F. N., M. Zhou, and A. Auerbach. 1999. A re-examination of adult mouse nicotinic acetylcholine receptor channel activation kinetics. *J. Physiol.* 516:315–330.

Sigworth, F., and S. M. Sine. 1987. Data transformation for improved display and fitting of single-channel dwell time histograms. *Biophys. J.* 52:1047–1052.

Sine, S. M. 1993. Molecular dissection of subunit interfaces in the acetylcholine receptor: identification of residues that determine curare selectivity. *Proc. Natl. Acad. Sci. U. S. A.* 90:9436–9440.

Sine, S. M., K. Ohno, C. Bouzat, A. Auerbach, M. Milone, J. N. Pruitt, and A. G. Engel. 1995. Mutation of the acetylcholine receptor alpha subunit causes a slow-channel myathenic syndrome by enhancing agonist-binding affinity. *Neuron.* 15:229–239.

Unwin, N. 1995. Acetylcholine receptor channel imaged in the open state. *Nature.* 373:37–43.

Wang, H-L., A. Auerbach, N. Bren, K. Ohno, A. G. Engel, and S. M. Sine. 1997. Mutation in the M1 domain of the acetylcholine receptor α subunit decreases the rate of agonist dissociation. *J. Gen. Physiol.* 109:757–766.

Wang, H-L., M. Milone, K. Ohno, X-M. Shen, A. Tsujino, A. P. Batocchi, P. Tonali, J. Brengman, A. G. Engel, and S. M. Sine. 1999. Acetylcholine receptor M3 domain: stereochemical and volume contributions to channel gating. *Nat. Neurosci.* 2:226–233.